Bioorganic & Medicinal Chemistry Letters 21 (2011) 5881–5887

Contents lists available at SciVerse ScienceDirect

Bioorganic & Medicinal Chemistry Letters

journal homepage: www.elsevier.com/locate/bmcl

Development of 2-substituted-*N*-(naphth-1-ylmethyl) and *N*-benzhydrylpyrimidin-4-amines as dual cholinesterase and Aβ-aggregation inhibitors: Synthesis and biological evaluation

Tarek Mohamed [a,b], Jacky C.K. Yeung [a,b], Praveen P.N. Rao [b,*]

[a] Department of Biology, University of Waterloo, Waterloo, Ontario, Canada N2L 3G1
[b] School of Pharmacy, Health Sciences Campus, University of Waterloo, Waterloo, Ontario, Canada N2L 3G1

ARTICLE INFO

Article history:
Received 4 July 2011
Revised 22 July 2011
Accepted 25 July 2011
Available online 30 July 2011

Keywords:
Cholinesterase inhibitors (ChEIs)
Acetylcholinesterase (AChE)
Butyrylcholinesterase (BuChE)
Human acetylcholinesterase (*h*AChE)
Structure-activity relationship (SAR)
Amyloid-β (Aβ)
5,5′-Dithiobis(2-nitrobenzoic acid) (DTNB)

ABSTRACT

A group of 2-substituted *N*-(naphth-1-ylmethyl)pyrimidin-4-amines (**6a**–**k**) and *N*-benzhydrylpyrimidin-4-amines (**7a**–**k**) in conjunction with varying steric and electronic properties at the C-2 position were designed, synthesized and evaluated as dual cholinesterase and amyloid-β (Aβ)-aggregation inhibitors. The naphth-1-ylmethyl compound **6f** (2-(4-cyclohexylpiperazin-1-yl)-*N*-(naphth-1-ylmethyl)pyrimidin-4-amine) exhibited optimum dual ChE (AChE IC_{50} = 8.0 μM, BuChE IC_{50} = 3.9 μM) and *h*AChE-promoted Aβ-aggregation inhibition (30.8% at 100 μM), whereas in the *N*-benzhydryl series, compound **7f** (*N*-benzhydryl-2-(4-cyclohexylpiperazin-1-yl)pyrimidin-4-amine) exhibited optimum combination of dual ChE (AChE IC_{50} = 10.0 μM, BuChE IC_{50} = 7.6 μM) and *h*AChE-promoted Aβ-aggregation inhibition (32% at 100 μM). These results demonstrate that a 2,4-disubstituted pyrimidine ring serves as a suitable template to target multiple pathological routes in AD, with a C-2 cyclohexylpiperazine substituent providing dual ChE inhibition and potency whereas a C-4 diphenylmethane substituent provides Aβ-aggregation inhibition.

Alzheimer's disease (AD) is a devastating neurodegenerative disease that targets the cholinergic regions of the central nervous system (CNS) associated with cognitive ability and spatial awareness.[1] The pathological initiation and progression of AD is highly complex and its prevalence is on the rise with significant socioeconomic impact that places a heavy burden on patients and their care providers.[2,3] Some molecular and physical characteristics of AD include the progressive loss of cholinergic neurons leading to cognitive dysfunction, the accelerated generation and aggregation of amyloid-β (Aβ) fibrils and the formation of neurofibrillary tangles (NFTs).[2–6] These findings support the basis for the cholinergic, amyloid and tau hypotheses of AD etiology.

The cholinergic dysfunction hypothesis attributes the pathology of AD to the systemic collapse of acetylcholine (ACh) mediated neurotransmission in the cortical regions of the CNS.[7] Its action in the synapse is terminated by cholinesterase enzymes; acetyl- and butyrylcholinesterase (AChE and BuChE), respectively.[8,9] Impairment of the ACh synthesizing enzyme (choline acetlytransferase – ChAT) in AD patients also contributes to the overall decline of ACh concentration in the CNS.[9–12] Furthermore, recent evidence suggests that AChE plays a vital role in the early stages of AD; however, as the disease progresses BuChE, with a wider distribution within the body, acts as the major ACh degrading enzyme indicating the need to develop dual AChE and BuChE inhibitors.[13,14]

According to the amyloid hypothesis, the accelerated generation of $Aβ_{1-40/42}$-peptides and their rapid oligomerization and aggregation to toxic Aβ-plaques is a major factor for AD etiology.[15–17] Furthermore, recent studies have implicated metal-ions[18–24] and the peripheral anionic site (PAS) of AChE with facilitating the aggregation of those Aβ-fibrils.[25–29] These multiple factors signify the need to develop small molecule therapies that could potentially target multiple pathways in AD pathology.

Research efforts aimed at developing cholinesterase inhibitors (ChEIs) has led to the development of several fused and nonfused ring systems with a wide range of inhibitory profiles. Some examples are tacrine (**1**),[30] donepezil (Aricept®, **2**), a piperidine-based AChE inhibitor[31] and propidium (**3**), a PAS specific AChE inhibitor (Fig. 1).[32] In addition, recent work by DeLisa et al. examined *s*-triazine based ring templates (**4**) for their ability to inhibit the aggregation of $Aβ_{1-42}$ plaques.[33] In this regard, we previously reported the design, synthesis and evaluation of a group of heterocyclic, nonfused small molecules based on a 2,4-disubstituted pyrimidine ring template with ChE and Aβ-aggregation inhibitory profiles.[34,35]

Herein we expand on our efforts with the development of 2-substituted-*N*-(naphth-1-ylmethyl)-pyrimidin-4-amines (**6a**–**k**)

* Corresponding author. Tel.: +1 519 888 4567x21317; fax: +1 519 888 7910.
E-mail address: praopera@uwaterloo.ca (P.P.N. Rao).

0960-894X/$ - see front matter © 2011 Elsevier Ltd. All rights reserved.
doi:10.1016/j.bmcl.2011.07.091

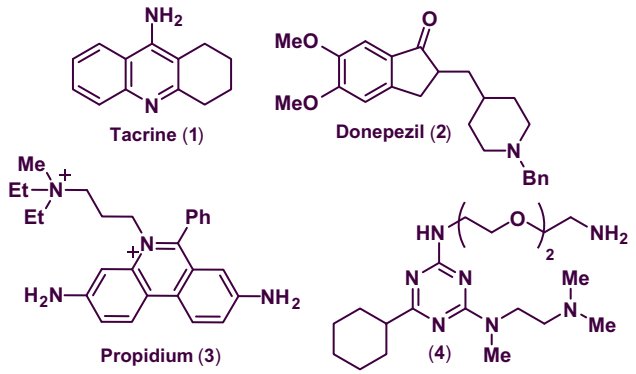

Figure 1. Structures of ChEIs (**1**, **2**) and Aβ-aggregation inhibitors (**3**, **4**).

and 2-substituted-*N*-benzhydrylpyrimidin-4-amines (**7a**–**k**) to explore their ChE and Aβ inhibitory potential.[36] In vitro ChE inhibition (ChEI)[37] and structure–activity relationship (SAR) data are discussed, along with their ability to inhibit *h*AChE-induced and self-induced aggregation of $A\beta_{1-40}$ fibrils[38] and some molecular modeling investigations on their binding modes are described.

The synthesis of target derivatives (**6a**–**k** and **7a**–**k**) was accomplished in two to three steps (Scheme 1). Initially, *N*-(naphth-1-ylmethyl)-2-chloropyrimidin-4-amine (**6**) and *N*-benzhydryl-2-chloropyrimidin-4-amine (**7**) intermediates were synthesized from the 2,4-dichloropyrimidine starting material (**5**) by a nucleophilic aromatic substitution reaction at the C-4 position using either napth-1-ylmethanamine or benzhydrylamine in presence of *N*,*N*-diisopropylethylamine (DIPEA). The reaction was run in EtOH at 80–85 °C and refluxed for 4 h. Intermediates **6** and **7** were obtained in moderate to good yields ranging from 55% to 75% (Scheme 1).[34,35,39] In the second step, the C-2 chlorine was displaced by various substituted cyclic amines (1-methylpiperazine, 4-methylpiperidine, *N*-isopropylpiperazine, 4-isopropylpiperidine, *N*-propylpiperazine, 1-cyclohexylpiperazine, 1-acetylpiperazine, *t*-butyl piperazine-1-carboxylate, *N*-(2-hydroxyethyl)piperazine or 1-(2-methoxyethyl)piperazine). This reaction was run in *n*-butanol under rigorous conditions (145–150 °C) for 50–60 min in a sealed pressure vessel (PV) to afford the target 2-substituted-*N*-(naphth-1-ylmethyl)pyrimidin-4-amines (**6a**–**k**) and 2-substituted-*N*-benzyhydrylpyrimidin-4-amines (**7a**–**k**) in moderate to good yield (50–80%) (Scheme 1).[34,35,40] The deprotection of the *tert*-butoxycarbonyl (*t*-Boc) group of **6h** [*tert*-butyl 4-(4-[(naphth-1-ylmethyl)amino]pyrimidin-2-yl)piperazine-1-carboxylate] and **7h** [*tert*-butyl 4-(4-[benzhydrylamino]pyrimidin-2-yl)piperazine-1-carboxylate] was accomplished using 50% v/v trifluoroacetic acid (TFA) to yield *N*-(naphth-1-ylmethyl)-2-(piperazin-1-yl)pyrimidin-4-amine (**6i**) and *N*-benzhydryl-2-(piperazin-1-yl)pyrimidin-4-amine (**7i**), respectively in good yield (60%) (Scheme 1).

The ChE inhibitory (ChEI) profiles of the 2,4-disubstituted pyrimidine derivatives (**6a**–**k** and **7a**–**k**) were determined using an in vitro assay based on a modified version of the Ellman protocol.[41] The IC_{50} values, selectivity index (S.I.), partition coefficient (*C* log *P*) and molecular volume ($Å^3$) are reported in Tables 1 and 2 along with tacrine (**1**), donepezil (**2**) and galantamine as controls. The SAR studies indicated that ChEI and selectivity were sensitive to the steric and electronic parameters at both C-2 and C-4 positions of the pyrimidine ring. These derivatives exhibited a broad range of inhibition (C-4 naphth-1-ylmethyl series, AChE IC_{50} = 8.0–50.8 μM range; BuChE IC_{50} = 2.2 to >100 μM range and C-4 *N*-benzhydryl series, AChE IC_{50} = 10.0 to >100 μM range; BuChE IC_{50} = 7.6 to >100 μM range).[35]

Among the naphth-1-ylmethyl series of derivatives (**6a**–**k**), the substituent electronic and steric properties at C-2 position modulated ChE inhibition (Table 1). The SAR of C-2 piperazine-substituted derivatives were explored by incorporating a wide range of terminal 4-alkyl, cycloalkyl, acyl and alkoxy substituents (**6a**, **c** and **e**–**k**). The presence of a methyl, isopropyl or *N*-propyl group in **6a**, **c** or **e** (X–R^2 = 1-methylpiperazine, *N*-isopropylpiperazine and *N*-propylpiperazine, respectively) provided equipotent AChE inhibitory activity (IC_{50} = 17.5, 15.8 and 19.0 μM, respectively). In contrast, BuChE inhibition and potency was dependent on the nature of the alkyl group attached. The presence of a smaller methyl group in **6a** provided potent and selective BuChE inhibition (IC_{50} = 2.6 μM), whereas the presence of a branched isopropyl in **6c** (IC_{50} = 7.6 μM) or *N*-propyl side chain in **6e** (IC_{50} = 18.1 μM) resulted in a ~threefold decrease in potency. Replacing the isopropyl group in **6c** with a cycloalkyl group as in **6f** (X–R^2 = 1-cyclohexylpiperazine) resulted in a ~twofold increase in both AChE and BuChE inhibitory potency (IC_{50} = 8.0 and 3.9 μM, respectively) relative to **6c**. In addition, **6f** exhibited near equipotent BuChE inhibition compared to the reference drug donepezil (IC_{50} = 3.6 μM). The

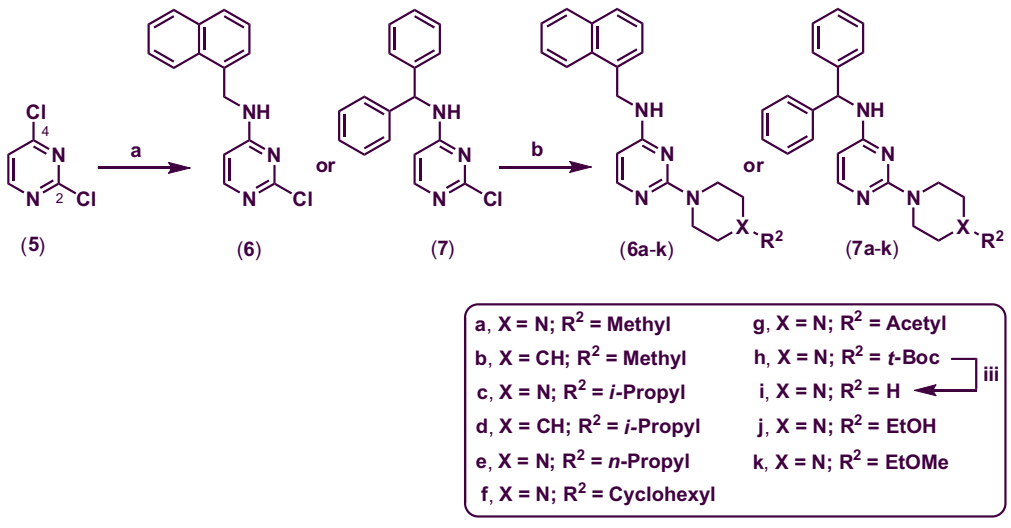

Scheme 1. Reagents and conditions: (a) DIPEA, naphth-1-ylmethanamine or diphenylamine, EtOH, 0 °C to 80–85 °C and reflux for 4 h; (b) various cyclic amines; 1-methylpiperazine, 4-methylpiperidine, *N*-isopropylpiperazine, 4-isopropylpiperidine, *N*-propylpiperazine, 1-cyclohexylpiperazine, 1-acetylpiperazine, *t*-butyl piperazine-1-carboxylate, *N*-(2-hydroxyethyl)piperazine or 1-(2-methoxyethyl)piperazine, respectively, *n*-BuOH, 145–150 °C, 50–60 min; (iii) TFA, CH_2Cl_2, 0 °C to rt, 2 h.

Table 1
ChEI activity profile, *C* log *P* and molecular volume data for compounds **6a–k**

Compound	IC_{50} (μM) ± SEM[a]		S.I.[b]	*C* log *P*[c]	Vol. (Å^3) [d]	X–R^2 group
	*h*AChE	*Eq*BuChE				
6a[35]	17.5 ± 1.8	2.6 ± 0.3	6.7	3.9	230	**N–Me**
6b[35]	25.8 ± 2.6	2.2 ± 0.2	11.7	5.2	232	**HC–Me**
6c	15.8 ± 2.1	7.6 ± 0.8	2.1	4.7	255	
6d	16.7 ± 1.7	9.1 ± 0.9	1.8	6.2	258	
6e	19.0 ± 1.9	18.1 ± 1.8	1.1	4.9	256	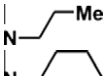
6f	8.0 ± 1.9	3.9 ± 0.4	2.1	5.8	284	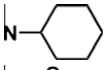
6g	13.8 ± 1.4	32.9 ± 0.4	0.4	2.9	244	
6h	50.8 ± 5.1	>100	<0.5	5.3	293	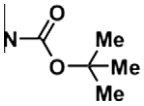
6i	17.5 ± 1.8	25.4 ± 8.9	0.7	3.3	216	**N–H**
6j	9.8 ± 0.8	17.9 ± 1.8	0.5	3.3	247	
6k	11.7 ± 2.5	26.5 ± 2.7	0.4	4.1	260	
Tacrine	0.077 ± 0.008	0.021 ± 0.001	3.4	3.3	138	(**1**)
Donepezil	0.032 ± 0.003	3.6 ± 0.4	0.009	4.6	271	(**2**)
Galantamine	3.2 ± 0.7	12.6 ± 1.3	0.3	1.0	179	–

[a] The in vitro test compound concentration required to produce 50% inhibition of *h*AChE and equine BuChE. The result (IC_{50}) is the mean of two separate experiments ($n = 4$).
[b] Selectivity Index = *h*AChE IC_{50}/BuChE IC_{50}.
[c] *C* log *P* was determined using ChemDraw Ultra 12.0. CambridgeSoft Company.
[d] Molecular volume (Å^3) was determined using a minimization protocol using the molecular properties calculator in the *Discovery Studio* program from Accelrys Inc. (San Diego, CA).

presence of polar groups such as a hydroxyethyl in **6j** (X–R^2 = *N*-(2-hydroxyethyl)piperazine; AChE IC_{50} = 9.8 μM; BuChE IC_{50} = 17.9 μM) or a methoxyethyl in **6k** (X–R^2 = 1-(2-methoxyethyl)piperazine; AChE IC_{50} = 11.7 μM; BuChE IC_{50} = 26.5 μM) resulted in better AChE inhibition compared to the alkyl-piperazines **6a**, **c** and **d** (Table 1). The introduction of an acetyl group in **6g** (X–R^2 = 1-acetylpiperazine; AChE IC_{50} = 13.8 μM; BuChE IC_{50} = 32.9 μM) resulted in AChE activity comparable to **6k** with a decrease in BuChE potency. In contrast the presence of a bulky *t*-Boc group in **6h** (X–R^2 = *tert*-butyl piperazine-1-carboxylate, molecular volume = 293 Å^3) led to a significant decrease in AChE potency (IC_{50} = 50.8) compared to all the other compounds from the naphth-1-ylmethyl series (Table 1). In addition, **6h** exhibited a loss of BuChE activity (IC_{50} >100 μM). Interestingly, once the *t*-Boc group was hydrolyzed to generate the free piperazine ring as in **6i** (X–R^2 = piperazine), dual ChE inhibition was restored (AChE IC_{50} = 17.5 μM; BuChE IC_{50} = 25.4 μM) and AChE potency was comparable to the methylated piperazine compound **6a** (AChE IC_{50} = 17.5 μM); however, **6i** exhibited a significant decrease in BuChE inhibitory potency compared to **6a** (BuChE IC_{50} = 2.6 μM). In addition, replacing the methylpiperazine group (**6a**) with a methylpiperidine bioisostere in **6b** provided comparable BuChE inhibition with greater selectivity (AChE IC_{50} = 25.8 μM; BuChE IC_{50} = 2.2 μM, S.I. = 11.7) relative to **6a**.[35] Furthermore, the bioisosteric replacement of C-2 isopropylpiperazine in **6c** with an isopropylpiperidine bioisostere in **6d** provided dual ChE inhibition similar to **6c** (AChE IC_{50} = 16.7 μM; BuChE IC_{50} = 9.1 μM).

In naphth-1-ylmethyl series, all the compounds evaluated (**6a–k**), except **6h** exhibited dual AChE and BuChE inhibition indicating that the presence of a C-4 naphth-1-yl group is a requirement to obtain dual ChE inhibition. In addition, the ChE inhibitory potency was sensitive to substituents at C-2 position. The cyclohexylpiperazine compound **6f** was identified as the most potent AChE inhibitor among this series (AChE IC_{50} = 8.0 μM) with dual ChE inhibition (BuChE IC_{50} = 3.9 μM). In addition, the presence of polar C-2 groups in **6j** and **k** provided better AChE inhibition. Furthermore, the presence of alkyl groups in **6a–d** at C-2 position within this series modulated ChE activity in favor of BuChE and the potency was of the order: 4-methylpiperidine **6b** >1-methylpiperazine **6a** >*N*-isopropylpiperazine **6c** >4-isopropylpiperidine **6d**. In addition, derivatives **6c**, **d** and **f** were ~1.5 to threefold more potent BuChE inhibitors compared to the reference compound galantamine (BuChE IC_{50} = 12.6 μM).

Among the *N*-benzhydryl series of derivatives (**7a–k**), the presence of a methyl or *N*-propyl group in **7a** or **e** (X–R^2 = 1-methylpiperazine or *N*-propylpiperazine, Table 2) provided similar AChE inhibitory activity (IC_{50} = 13.7 and 14.6 μM, respectively); however, **7a** was less potent as a BuChE inhibitor compared to **7e** (IC_{50} = 23.8 and 17.5 μM, respectively). Replacing the *N*-propyl chain with the branched isopropyl group in **7c** (X–R^2 = *N*-isopropylpiperazine) resulted in a ~1.4-fold decrease in AChE potency and a ~1.8-fold increase in BuChE potency (IC_{50} = 20.3 and 9.7 μM, respectively) relative to **7e**. When compared to **7a**, the isopropyl derivative (**7c**) exhibited a ~1.5-decrease in AChE potency and a ~2.5-fold increase in BuChE potency. The presence of a bulkier cycloalkyl group as in **7f** (X–R^2 = 1-cyclohexylpiperazine, molecular volume = 303 Å^3, Table 2) resulted in a ~twofold increase in AChE potency and a ~1.3-fold increase in BuChE potency (AChE IC_{50} = 10.0 and BuChE IC_{50} 7.6 μM, respectively) relative to **7c** and was the most potent dual ChE inhibitor in the *N*-benzhydryl

Table 2
ChEI activity profile, *C* log *P* and molecular volume data for compounds **7a–k**

Compound	IC_{50} (μM) ± SEM[a]		S.I.[b]	*C* log *P*[c]	Vol. (Å^3) [d]	X–R^2 group
	AChE	BuChE				
7a	13.7 ± 1.4	23.8 ± 2.4	0.6	4.1	248	**N–Me**
7b	32.2 ± 5.4	33.8 ± 1.6	0.9	5.4	251	**HC–Me**
7c	20.3 ± 2.1	9.7 ± 1.0	2.1	4.9	279	
7d	42.5 ± 4.3	87.0 ± 8.7	0.5	6.3	282	
7e	14.6 ± 1.5	17.5 ± 1.8	0.8	5.1	272	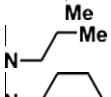
7f	10.0 ± 0.9	7.6 ± 0.1	1.3	6.0	303	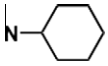
7g	29.0 ± 2.9	>100	<0.3	3.1	260	
7h	>100	>100	–	5.5	311	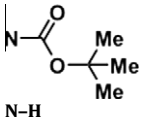
7i	31.3 ± 3.1	>100	<0.3	3.5	235	**N–H**
7j	21.6 ± 2.2	59.5 ± 6.0	0.4	3.5	265	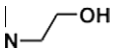
7k	39.2 ± 3.9	28.4 ± 2.8	1.4	4.2	285	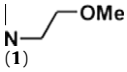
Tacrine	0.077 ± 0.008	0.021 ± 0.001	3.4	3.3	138	(**1**)
Donepezil	0.032 ± 0.003	3.6 ± 0.4	0.009	4.6	271	(**2**)
Galantamine	3.2 ± 0.7	12.6 ± 1.3	0.3	1.0	179	–

[a] The in vitro test compound concentration required to produce 50% inhibition of *h*AChE and equine BuChE. The result (IC_{50}) is the mean of two separate experiments ($n = 4$).
[b] Selectivity Index = *h*AChE IC_{50}/BuChE IC_{50}.
[c] *C* log *P* was determined using ChemDraw Ultra 12.0. CambridgeSoft Company.
[d] Molecular volume (Å^3) was determined using a minimization protocol using the molecular properties calculator in the *Discovery Studio* program from Accelrys Inc. (San Diego, CA).

series. When compared to the *N*-propyl group in **7e** (AChE IC_{50} = 14.6 μM; BuChE IC_{50} = 17.5 μM), the presence of polar groups such as a hydroxyethyl in **7j** (X–R^2 = 2-hydroxyethylpiperazine; AChE IC_{50} = 21.6 μM; BuChE IC_{50} = 59.5 μM) or a methoxyethyl in **7k** (X–R^2 = 2-methoxyethylpiperazine; AChE IC_{50} = 39.2 μM; BuChE IC_{50} = 28.4 μM) resulted in reduced ChE inhibitory potency. On the other hand, the introduction of an acetyl group in **7g** (X–R^2 = 1-acetylpiperazine; AChE IC_{50} = 29.9 μM; BuChE IC_{50} >100 μM) resulted in moderate AChE activity and led to a loss of BuChE activity. The presence of a bulky *t*-Boc group in **7h** (X–R^2 = *tert*-butyl piperazine-1-carboxylate) led to a loss of ChE activity (IC_{50} >100 μM). Interestingly, once the *t*-Boc group was hydrolyzed to generate the free piperazine ring as in **7i** (X–R^2 = piperazine), AChE inhibition was restored (AChE IC_{50} = 31.3 μM) although **7i** did not exhibit BuChE inhibition (IC_{50} >100 μM). In addition, replacing the methylpiperazine group (**7a**) with a methylpiperidine bioisostere in **7b** resulted in a dual, nonselective ChE inhibitory profile (AChE IC_{50} = 32.2 μM; BuChE IC_{50} = 33.8 μM, S.I. ~1.0) relative to **7a**. Furthermore, the bioisosteric replacement of C-2 isopropylpiperazine in **7c** with corresponding isopropylpiperidine bioisostere in **7d** resulted in a ~twofold decrease in AChE potency and weak BuChE inhibition (AChE IC_{50} = 42.5 μM; BuChE IC_{50} = 87.0 μM) compared to **7c**.

It is noteworthy that the molecular volumes (Å^3) of *N*-benzhydryl derivatives (**7a–k**) are ~6–9% greater than those of their naphth-1-ylmethyl derivatives (**6a–k**) (Tables 1 and 2). The majority of *N*-benzhydryl derivatives were not as potent as their naphth-1-ylmethyl derivatives with the exception of **7a** and **e** (~1.3-fold increase in AChE inhibition compared to **6a** and **e**, respectively). Compound **7c** was identified as a selective BuChE inhibitor with ~1.3-fold greater potency against BuChE compared to galantamine (BuChE IC_{50} = 12.6 μM). Derivative **7f** with a C-2 cyclohexylpiperazine was identified as the most potent dual ChE inhibitor (AChE IC_{50} = 10.0 and BuChE IC_{50} 7.6 μM; S.I. = 1.3) with slight selectivity toward BuChE. It was interesting to note that the presence of a C-2 cyclohexylpiperazine substituent in both naphth-1-ylmethyl (**6f**) and *N*-benzhydryl series (**7f**) provided ChE inhibition and superior potency for both AChE and BuChE, indicating that a C-2 cyclohexylpiperazine substituent could be a potential ChE pharmacophore for 2,4-disubstituted pyrimidines.

The ability of naphth-1-ylmethyl and *N*-benzhydrylpyrimidin-4-amines (**6a–k** and **7a–k**) to prevent both *h*AChE-induced and self-induced $A\beta_{1-40}$ aggregation was evaluated by a thioflavin T (ThT) fluorescence assay (Table 3).[35] In the *h*AChE-induced aggregation assay, the anti-$A\beta_{1-40}$ aggregation activity ranged from no activity to 31.8% inhibition. Among the naphth-1-ylmethyl series of compounds (**6a–k**), the presence of a C-2 *N*-isopropylpiperazine (**6c**), *N*-propylpiperazine (**6e**), cyclohexylpiperazine (**6f**) and 2-hydroxyethylpiperazine (**6j**) provided inhibition of *h*AChE-induced $A\beta_{1-40}$ aggregation. Compound **6f** exhibited superior inhibition (30.8% inhibition at 100 μM) compared to **6c**, **e** and **j** and was less potent compared to propidium (82% at 100 μM). It is interesting to note that **6f** is the most potent AChE inhibitor (IC_{50} = 8.0 μM) in the naphth-1-ylmethyl series, which supports its ability to inhibit PAS mediated $A\beta_{1-40}$ aggregation. This is further supported by the fact that **6f** was not active in the self-induced $A\beta_{1-40}$ aggregation assay (Table 3). These studies indicate that for the naphth-1-ylmethyl series of compounds, the *h*AChE-induced aggregation inhibition is sensitive to the steric and electronic factors of substituents at the C-2 position of the pyrimidine ring. In the *N*-benzhydryl series

Table 3
Percent inhibition of *h*AChE-induced and self-induced $A\beta_{1-40}$ aggregation by **6a–k** and **7a–k** at 100 M

Compound	Inhibition of $A\beta_{1-40}$ aggregation (%) ± SD[a]	
	*h*AChE-induced	Self-induced
6a	NA	NA
6b	NA	NA
6c	17.1 ± 1.7	12.1 ± 1.2
6d	NA	NA
6e	22.0 ± 2.2	NA
6f	30.8 ± 3.1	NA
6g	NA	NA
6h	NA	NA
6i	NA	NA
6j	13.4 ± 1.3	NA
6k	NA	NA
7a	24.1 ± 2.4	24.8 ± 1.2
7b	14.8 ± 1.4	18.9 ± 1.9
7c	20.8 ± 2.1	21.8 ± 2.2
7d	31.8 ± 3.2	11.8 ± 1.2
7e	23.1 ± 2.3	18.2 ± 1.8
7f	32.0 ± 3.2	27.6 ± 2.8
7g	10.3 ± 1.0	15.8 ± 1.6
7h	13.6 ± 1.4	11.4 ± 1.1
7i	NA	20.8 ± 2.1
7j	18.8 ± 1.9	15.0 ± 1.5
7k	10.4 ± 1.0	16.3 ± 1.6
Propidium iodide	82.1 ± 8.2	ND
Donepezil. HCl	17.0 ± 1.7[b]	ND
Galantamine. HBr	ND	~48[c]

[a] The result (% inhibition) is the mean of two separate experiments ($n = 4$).
[b] Previously reported [Ref. 35].
[c] Previously reported [Ref. 45], NA, not active; SD, standard deviation; ND, not determined.

(**7a–k**), it was interesting to note that all the compounds except **7i** exhibited activity in both *h*AChE-promoted as well as self-induced $A\beta_{1-40}$ aggregation assay (inhibition range ~10–32%) (Table 3). This clearly indicates that the presence of a C-4 diphenylmethane group is a major contributing factor involved in the inhibition $A\beta_{1-40}$ aggregation. Compounds **7d** (4-isopropylpiperidine) and **f** (cyclohexylpiperazine) exhibited almost equipotent inhibition of $A\beta_{1-40}$ aggregation (~32% inhibition toward *h*AChE-induced Aβ-aggregation). These observations indicate the effect of C-4 aromatic ring structures on $A\beta_{1-40}$ aggregation. For example, a C-4 diphenylmethane substituent could potentially interact with $A\beta_{1-40}$ peptides and prevent them from stacking/aggregating and could serve as a suitable pharmacophore to prevent both self-induced as well as *h*AChE-induced $A\beta_{1-40}$ aggregation as compared to a planar C-4 naphth-1-yl substituent. Furthermore, the ability of synthesized compounds to reach the central nervous system was correlated by calculating the theoretical *C* log *P* values (Tables 1 and 2). They exhibited a wide range from 2.9 to 6.3. In this regard, compound **6f** that exhibited a good combination of dual ChE and Aβ-aggregation inhibition exhibited a *C* log *P* value of 5.8 which is comparable with the marketed anti-AD compound donepezil (*C* log *P* = 4.6) indicating it's potential to reach the central nervous system.

The ligand-enzyme binding interactions of the potent dual ChE inhibitor, **6f** (*h*AChE IC_{50} = 8.0 μM; equine serum BuChE IC_{50} = 3.9 μM, S.I. = 2.1), were investigated by molecular modeling studies. The docking study of **6f** within the active site of *h*AChE (Fig. 2) indicates that the pyrimidine ring was positioned midway through the active site gorge (~8.0 Å away from the catalytic triad His447 residue at the bottom of the active site and ~7.0 Å away from the gorge entry, with *N*-3 oriented toward the entry). The ring was stacked close to Phe295, Phe297 and Phe338 (distance ~4.5–7.5 Å). The C-4 naphth-1-yl ring was stacked between Trp86 and a tyrosine pocket comprised of Tyr124, Tyr337 and Tyr341 (distance ~3.8–5.8 Å). The C-4 N*H* group was undergoing hydrogen bonding with the hydroxyl group of Tyr124 (distance ~2.9 Å) and the O*H* of Tyr124 was also undergoing hydrogen bonding interaction with the C-4 pyrimidin-4-amine nitrogen (distance ~3.1 Å). The cyclohexylpiperazine C-2 group of **6f** was oriented toward the PAS, where the cyclohexyl ring was perpendicularly stacked over Trp286 (distance ~4.1 Å) and was ~4.8 Å away from Leu289. The piperazine ring was stacked over Ser293 and Val294 (distance ~4.7 Å). It is significant to note that the linear conformation allows **6f**, to span both the catalytic active site (CAS) and PAS that contributes to its superior binding to *h*AChE. In general the molecular volumes of naphth-1-ylmethyl derivatives were ~6–9%

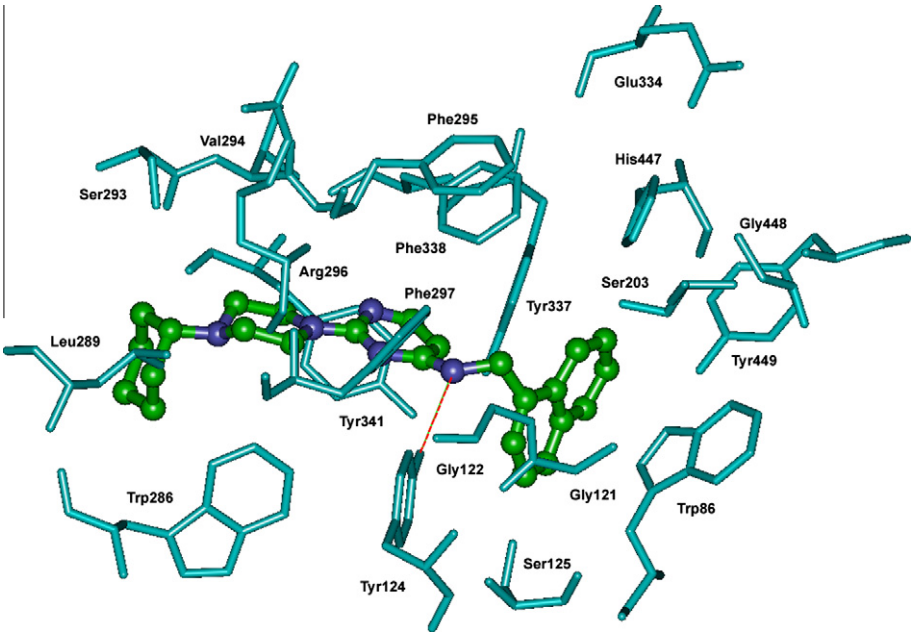

Figure 2. Docking of 2-(4-cyclohexylpiperazin-1-yl)-*N*-(naphth-1-ylmethyl)pyrimidin-4-amine (**6f**) in the active site of *h*AChE (PBD code: 1B41). Red lines represent hydrogen-bond interactions. Hydrogen atoms are not shown for clarity.

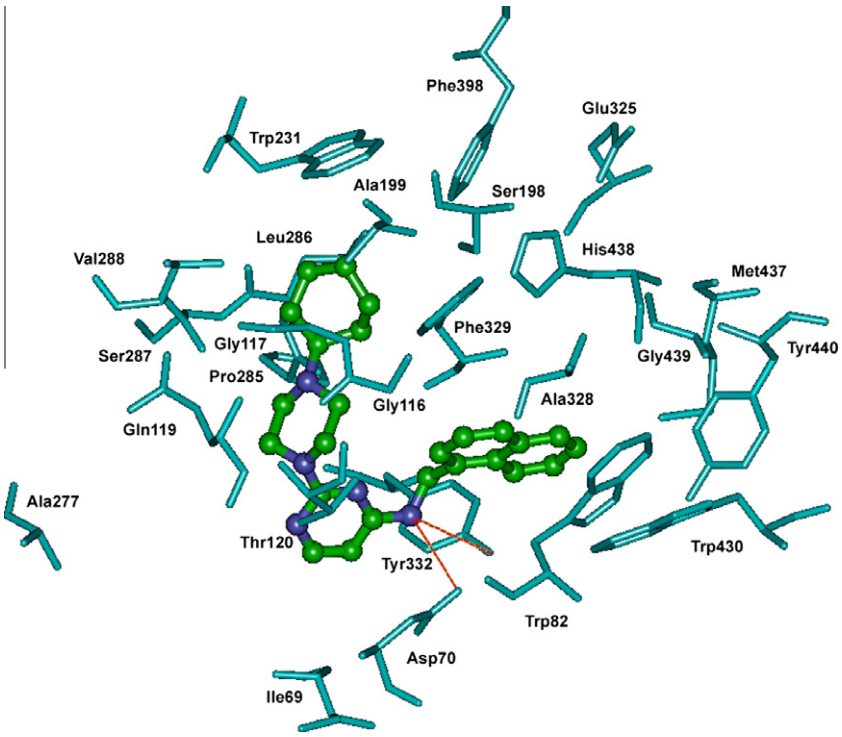

Figure 3. Docking of 2-(4-cyclohexylpiperazin-1-yl)-*N*-(naphth-1-ylmethyl)pyrimidin-4-amine (**6f**) in the active site of *h*BuChE (PBD code: 1P0I). Red lines represent hydrogen-bond interactions. Hydrogen atoms are not shown for clarity.

smaller ($Å^3$) compared to their *N*-benzhydryl counterparts **7a–k** and this resulted in better anti-ChE profile for the naphth-1-ylmethyl derivatives.

On the other hand, the docking study of **6f** within the active site of *h*BuChE (Fig. 3) indicates that the pyrimidine ring was positioned midway through the active site gorge (~9.1 Å away from the catalytic triad His438 residue at the bottom of the active site and ~9.5 Å away from the gorge entry) with *N*-1 directly facing Ala277 at the active site entrance. The pyrimidine ring was stacked between Pro285 and Ile69/Asp70 (distance ~8.0 and ~4.4 Å, respectively). The C-4 naphth-1-yl ring was stacked between Trp82 and Phe329 (distance ~4.2 and 6.0 Å, respectively) and positioned in an aromatic pocket comprised of Trp430 (distance ~4.4 Å), Tyr440 (distance ~5.3 Å) and Tyr332 (distance ~3.9 Å). The C-4 N*H* group was undergoing hydrogen bonding with the *O*H group of Tyr332 (distance ~3.1 Å) and the COOH side chain of Asp70 (distance ~3.1 Å). The cyclohexylpiperazine C-2 group of **6f** was oriented toward a hydrophobic pocket, where the piperazine ring was in close proximity to Gly116/117, Gln119 and Thr120 (distance <5.0 Å) and the cyclohexyl ring was in close proximity to Ser198, Trp231, Leu286, Ser287, Val288 and Phe398 (distance <5.0 Å). Although the overall U-shape conformation of **6f** in BuChE does not facilitate multiple hydrogen bonds, the strong hydrophobic interactions with the C-2 group and the positioning of the C-4 naphth-1-yl ring in close proximity to Trp82 contributes its superior binding toward BuChE.

In conclusion, our studies indicate that the presence of a C-4 naphth-1-ylmethyl substituent generally provides dual AChE and BuChE inhibitors with **6f** (2-(4-cyclohexylpiperazin-1-yl)-*N*-(naphth-1-ylmethyl)pyrimidin-4-amine) exhibiting optimum dual ChE (AChE IC_{50} = 8.0 μM, BuChE IC_{50} = 3.9 μM) and *h*AChE-promoted Aβ-aggregation inhibition (30.8% at 100 μM), whereas the presence of a C-4 diphenylmethane substituent generally led to a loss in ChE inhibitory potency, with a gain in both *h*AChE-promoted and self-induced Aβ-aggregation inhibition. Among the *N*-benzhydryl series, compound **7f** (*N*-benzhydryl-2-(4-cyclohexylpiperazin-1-yl)pyrimidin-4-amine) exhibited optimum combination of dual ChE (AChE IC_{50} = 10.0 μM, BuChE IC_{50} = 7.6 μM) and *h*AChE-promoted Aβ-aggregation inhibition (32% at 100 μM). Results of the biological screening and SAR studies demonstrate that the 2,4-disubstituted pyrimidine ring could potentially serve as a suitable template to design small molecules that could target multiple pathological routes in AD, such as dual inhibition of AChE and BuChE, coupled with anti-Aβ-aggregation activity.

Acknowledgments

The authors would like to thank the Department of Biology and the School of Pharmacy at the University of Waterloo for supporting this research project.

Supplementary data

Supplementary data associated with this article can be found, in the online version, at doi:10.1016/j.bmcl.2011.07.091.

References and notes

1. Holden, M.; Kelly, C. *Adv. Psychiatr. Treat.* **2002**, *8*, 89.
2. Klafki, H.; Staufenbiel, M.; Kornhuber, J.; Wiltfang, J. *Brain* **2006**, *129*, 2840.
3. Edwards, P. D.; Albert, J. S.; Sylvester, M.; Aharony, D.; Andisik, D.; Callaghan, O.; Campbell, J. B.; Carr, R. A.; Chessari, G.; Congreve, M.; Frederickson, M.; Folmer, R. H. A.; Geschwindner, S.; Koether, G.; Kolmodin, K.; Krumrine, J.; Mauger, R. C.; Murray, C. W.; Olsson, L.; Patel, S.; Spear, N.; Tian, G. *J. Med. Chem.* **2007**, *50*, 5912.
4. Selkoe, D. J. *Science* **2002**, *298*, 789.
5. Aguzzi, A.; O'Conner, T. *Nat. Rev. Drug Disc.* **2010**, *9*, 237.
6. Melnikova, I. *Nat. Rev. Drug Disc.* **2007**, *6*, 341.
7. Suh, W. H.; Suslick, K. S.; Suh, Y. *Curr. Med. Chem.* **2005**, *5*, 259.
8. Shen, T.; Tai, K.; Henchman, R. H.; McCammon, J. A. *Acc. Chem. Res.* **2002**, *35*, 332.
9. Darvesh, S.; Hopkins, D. A.; Geula, C. *Nat. Rev. Neurosci.* **2003**, *4*, 131.
10. Green, K. D.; Fridman, M.; Garneau-Tsodikova, S. *ChemBioChem* **2009**, *10*, 2191.

11. Soreq, H.; Seidman, S. *Nat. Rev. Neurosci.* **2001**, *2*, 294.
12. Villalobos, A.; Blake, J. F.; Biggers, C. K.; Butler, T. W.; Chapin, D. S.; Chen, Y. L.; Ives, J. L.; Jones, S. B.; Liston, D. R.; Nagel, A. A.; Nason, D. M.; Neilson, J. A.; Shalaby, I. A.; White, W. F. *J. Med. Chem.* **1994**, *37*, 2721.
13. Kamal, M. A.; Qu, X.; Yu, Q.; Tweedie, D.; Holloway, H. W.; Li, Y.; Tan, Y.; Greig, N. H. *J. Neural. Transm.* **2008**, *115*, 889.
14. Campiani, G.; Fattorusso, C.; Butini, S.; Gaeta, A.; Agnusdei, M.; Gemma, S.; Persico, M.; Catalanotti, B.; Savini, L.; Nacci, V.; Novellino, E.; Holloway, H. W.; Greig, N. H.; Belinskaya, T.; Fedorko, J. M.; Saxena, A. *J. Med. Chem.* **2005**, *48*, 1919.
15. Gibbs, M. E.; Maksel, D.; Gibbs, Z.; Hou, X.; Summers, R. J.; Small, D. H. *Neurobiol. Aging* **2010**, *31*, 614.
16. Dinamarca, M. C.; Sagal, J. P.; Quintanilla, R. A.; Godoy, J. A.; Arrazola, M. S.; Inestrosa, N. C. *Mol. Neurodegener.* **2010**, *5*, 4.
17. Rosini, M.; Simoni, E.; Bartolini, M.; Cavalli, A.; Ceccarini, L.; Pascu, N.; McClymont, D. W.; Tarozzi, A.; Bolognesi, M. L.; Minarini, A.; Tumiatti, V.; Andrisano, V.; Mellor, I. R.; Melchiorre, C. *J. Med. Chem.* **2008**, *51*, 4381.
18. Karr, J. W.; Akintoye, H.; Kaupp, L. J.; Szalai, V. A. *Biochemistry* **2005**, *44*, 5478.
19. Chen, T.; Wang, X.; He, Y.; Zhang, C.; Wu, Z.; Liao, K.; Wang, J.; Guo, Z. *Inorg. Chem.* **2009**, *48*, 5801.
20. Smith, D. P.; Ciccotosto, G. D.; Tew, D. J.; Fodero-Tavoletti, M. T.; Johanssen, T.; Masters, C. L.; Barnham, K. J.; Cappi, R. *Biochemistry* **2007**, *46*, 2881.
21. Nakamura, M.; Shishido, N.; Nunomura, A.; Smith, M. A.; Perry, G.; Hayashi, Y.; Nakayama, K.; Hayashi, T. *Biochemistry* **2007**, *46*, 12737.
22. Sarell, C. J.; Syme, C. D.; Rigby, S. E. J.; Viles, J. H. *Biochemistry* **2009**, *48*, 4388.
23. Ha, C.; Ryu, J.; Park, C. B. *Biochemistry* **2007**, *46*, 6118.
24. Scott, L. E.; Orvig, C. *Chem. Rev.* **2009**, *109*, 4885.
25. Pakaski, M.; Kalman, J. *Neurochem. Int.* **2008**, *53*, 103.
26. Racchi, M.; Mazzucchelli, M.; Lenzken, S. C.; Porrello, E.; Lanni, C.; Govoni, S. *Chem. Biol. Interact.* **2005**, *157–158*, 335.
27. Inestrosa, N. C.; Dinamarca, M. C.; Alvarez, A. *FEBS* **2008**, *275*, 625.
28. Inestrosa, N. C.; Alvarez, A.; Perez, C. A.; Moreno, R. D.; Vincete, M.; Linker, C.; Casanueva, O. I.; Soto, C.; Garrido, J. *Neuron* **1996**, *16*, 881.
29. Belluti, F.; Rampa, A.; Piazzi, L.; Bisi, A.; Gobbi, S.; Bartolini, M.; Andrisano, V.; Cavalli, A.; Recanatini, M.; Valenti, P. *J. Med. Chem.* **2005**, *48*, 4444.
30. Harel, M.; Schalk, I.; Ehret-Sabatier, L.; Bouet, F.; Goeldner, M.; Hirth, C.; Axelsen, P. H.; Silman, I.; Sussman, J. L. *Proc. Natl. Acad. Sci. U.S.A.* **1993**, *90*, 9031.
31. Greenblatt, H. M.; Silman, I.; Sussman, J. L. *Drug Dev. Res.* **2000**, *50*, 573.
32. Bolognesi, M. L.; Andrisano, V.; Bartolini, M.; Banzi, R.; Melchiorre, C. *J. Med. Chem.* **2005**, *48*, 24.
33. Lee, L. L.; Ha, H.; Chang, Y.; Delisa, M. P. *Protein Sci.* **2009**, *18*, 277.
34. Mohamed, T.; Rao, P. P. N. *Bioorg. Med. Chem. Lett.* **2010**, *20*, 3606.
35. Mohamed, T.; Zhao, X.; Habib, L. K.; Yang, J.; Rao, P. P. N. *Bioorg. Med. Chem.* **2011**, *19*, 2269.
36. *General procedure for the synthesis of 4-substituted-2-chloropyrimidin-4-amines* (**6**–**7**)*:* To a mixture of 2,4-dichloropyrimidine (**5**) (5.00 g, 33.60 mmol) and primary amines (R^1 = naphth-1-ylmethanamine and diphenylmethanamine; 33.60 mmol) in 65 mL of EtOH, kept at 0 °C (ice-bath), DIPEA (6.08 mL, 36.80 mmol) was added. The reaction was allowed to stir on the ice-bath for 5 min and was refluxed at 80–85 °C for 4 h. After cooling to 25 °C, 20 mL of EtOAc was added and solution was neutralized with drop-wise addition of ~6 M HCl (pH = 7–7.5), washed with a saturated $NaHCO_3$ and NaCl solution (1 × 50 mL). Aqueous layer was re-washed with EtOAc (3 × 25 mL) and the combined organic layer was dried over anhydrous $MgSO_4$ and filtered. The organic layer is evaporated in vacuo and the resulting residue was further purified using either one or both of the following methods: (1) Method A: Silica gel column chromatography using EtOAc: hexanes twice (3:1 and 1:3 v/v, respectively) or 9:1 DCM: EtOAc to afford solid products (60–65%); (2) Method B: The collected organic layers were evaporated in vacuo and the oily residue was vigorously mixed with a solution of hexanes to afford a precipitate that was dried on filter paper at 80–85 °C for ~2–3 h to afford solid products.
General procedure for the synthesis of 2,4-disubstituted-pyrimidin-4-amines (**6a**–**k** and **7a**–**k**): To a solution of **6** or **7** (0.68–0.74 mmol) in 3 mL of *n*-BuOH kept in a PV with stirring, cyclic amines (1.02–1.11 mmol) was added. The sealed PV was placed in an oil bath at 145–150 °C and stirred for 50–60 min. The solvent was evaporated in vacuo with the aid of DCM and the residue was re-dissolved in 2:1 EtOAc/DCM and washed successively with saturated $NaHCO_3$ and NaCl solution (1 × 15 mL), respectively. The aqueous layer was washed with EtOAc (3 × 5 mL) and the organic layer was dried over anhydrous $MgSO_4$ then filtered. The solution was evaporated in vacuo and purified using silica gel column chromatography with appropriate eluents (EtOAc/hexanes 3:1 and 1:3 v/v, respectively or 9:1 DCM/EtOAc) to afford either solid or semisolid products.
General method for the preparation of 4-substituted-2-(piperazin-1-yl)pyrimidin-4-amine (**6i**, **7i**)**:** To a mixture of **6h** or **7h** (0.15 g, 0.33–0.36 mmol) in 5 mL of DCM, kept at 0 °C (ice-bath), TFA (5 mL, 67.29 mmol) was added drop wise. The reaction was allowed to stir on the ice-bath for 5 min and then was kept at rt for 2 h. DCM was evaporated in vacuo and the residue was re-dissolved in 1:1 EtOAc/DCM and successfully washed with saturated $NaHCO_3$ and NaCl solution (1 × 15 mL), respectively. Aqueous layer was washed with 1:1 EtOAc/DCM (3 × 15 mL) and the combined organic layer was dried over anhydrous $MgSO_4$ and filtered. The organic layer was evaporated in vacuo to afford solid products.
Analytical data for N-benzhydryl-2-(4-cyclohexylpiperazin-1-yl)pyrimidin-4-amine (**7f**). The product was obtained after coupling **7** with cyclohexylpiperazine (0.17 g, 1.02 mmol). The residue was purified using a 3:1 EtOAc/DCM column to afford a light yellow solid (0.17 g, 60%). mp: 53–55 °C. IR (film, $CDCl_3$): 3424 cm^{-1} (NH); ^1H NMR (300 MHz, $CDCl_3$) δ 7.83 (d, J = 6.0 Hz, 1H), δ 7.24–7.33 (m, 10H), δ 5.92 (br s, 1H), δ 5.61 (d, J = 6.0 Hz, 1H), δ 5.14 (br s, 1H), δ 3.64–3.68 (m, 4H), δ 2.49–2.52 (m, 4H), δ 2.27–2.32 (m, 1H), δ 1.81–1.86 (m, 2H), δ 1.75–1.80 (m, 2H) δ 1.60–1.64 (m, 1H), δ 1.21–1.27 (m, 5H). HREIMS Calcd for $C_{27}H_{33}N_5$ (M^+) m/z 427.5844, found 427.2733.
37. *Cholinesterase inhibition assay:* The ChE inhibition assay is based on the use of thio derivatives of ACh and BuCh and 5,5′-dithiobis-(2-nitrobenzoic acid) (DTNB) to generate a yellow chromophore (5-mercapto-2-nitrobenzoic acid) detectable at the 405–412 nm range. The assay was carried out as per a previously described protocol (Ref. 34,35) using tacrine hydrochloride, donepezil hydrochloride monohydrate and galantamine hydrobromide as controls (n = 4). Percent inhibition was calculated by the comparison of compound-treated to various control incubations and the concentration of the test compound causing 50% inhibition (IC_{50} μM) was calculated from the log concentration-log% inhibition response curve.
38. *hAChE-induced and self-induced $A\beta_{1-40}$ aggregation inhibition assay:* The thioflavin T (ThT) method was used to detect amyloid oligomers and fibrils.[42–44] The $A\beta_{1-40}$ HFIP was purchased from Anaspec (Cat. 64128-1), human recombinant AChE lyophilized powder and ThT were purchased from Sigma (Cat. C1682 and T3516; respectively) and the *h*AChE-induced assay was run using propidium iodide as a control. $A\beta_{1-40}$ was dissolved in DMSO and sonicated for 30 min to obtain a 232 μM solution. *h*AChE was dissolved in 215 mM sodium phosphate buffer (pH 8.0) to obtain a 4.69 μM solution. For the *h*AChE-induced assay, 4 μL of $A\beta_{1-40}$ were incubated with 20 μL of *h*AChE to give a final concentration of 23.2 μM of $A\beta_{1-40}$ and 2.35 μM of *h*AChE. For co-incubation experiments, 16 μL of test samples (100 μM) in 215 mM sodium phosphate buffer pH 8.0 solution (6% DMSO) were used. For the self-induced assay, 4 μL of $A\beta_{1-40}$ were incubated with 16 μL of test samples (100 μM) in 215 mM sodium phosphate buffer pH 8.0 solution (6% DMSO). 96-well plates were incubated at room temperature for 24 h and 150 μL of 15 μM of thioflavin T in 50 mM glycine-NaOH buffer (pH 8.5) was added. Fluorescence was monitored at 446 nm and emission 490 nm using a Molecular Devices SpectraMax spectrofluorometer. The fluorescence intensities in the presence and absence of inhibitors before and after the incubation period were compared and the percentage inhibition was calculated with equation: 100% control value (i.e. no inhibitor) – $[(IF_i–IF_o)]$ where IF_i and IF_o are the fluorescence intensities in the presence of ThT and absence of ThT before 24 h incubation, respectively.[35]
39. Nugiel, D. A.; Cornelius, L. A. M.; Corbett, J. W. *J. Org. Chem.* **1997**, *62*, 201.
40. Fiorini, M. T.; Abell, C. *Tetrahedron Lett.* **1998**, *39*, 1827.
41. Ellman, G. L.; Courtney, K. D.; Andres, V., Jr.; Featherstone, R. M. *Biochem. Pharmacol.* **1961**, *7*, 88.
42. Zhao, X.; Yang, J. *ACS Chem. Neurosci.* **2010**, *1*, 655.
43. Khurana, R.; Coleman, C.; Ionescu-Zanetti, C.; Carter, S. A.; Krishna, V.; Grover, R. K.; Roy, R.; Singh, S. *J. Struc. Biol.* **2005**, *151*, 229.
44. Eubanks, L. M.; Rogers, C. J.; Beuscher IV, A. E.; Koob, G. F.; Olson, A. J.; Dickerson, T. J.; Janda, K. D. *Mol. Pharmaceut.* **2006**, *3*, 773.
45. Matharu, B.; Gibson, G.; Parsons, R.; Huckerby, T. N.; Moore, S. A.; Cooper, L. J.; Millichamp, R.; Allsop, D.; Austen, B. *J. Neurol. Sci.* **2009**, *280*, 49.